Microchimica Acta (2020) 187: 181
https://doi.org/10.1007/s00604-020-4152-8

REVIEW ARTICLE

Recent advancements in fabrication of nanomaterial based biosensors for diagnosis of ovarian cancer: a comprehensive review

Rinky Sha [1] · Sushmee Badhulika [1]

Received: 25 November 2019 / Accepted: 2 February 2020 / Published online: 19 February 2020

Abstract

Ovarian cancer is commonly diagnosed via determination of biomarkers like CA125, Mucin 1, HE4, and prostasin that can be present in the blood. However, there is a substantial need for less expensive, simpler, and portable diagnostic tools, both for timely diagnosis and management of ovarian cancer. This review (with 101 refs.) discusses various kinds of nanomaterial-based biosensors for tumor markers. Following an introduction into the field, a first section covers different kinds of biomarkers for ovarian cancer including CA125 (MUC16), mucin 1 (MUC1), human epididymis protein 4 (HE4), and prostasin. This is followed by a short overview on conventional diagnostic approaches. A large section is then presented on biosensors for determination of ovarian cancer, with subsections on optical biosensors (fluorimetric, colorimetric, surface plasmon resonance, chemiluminescence, electrochemiluminescence), on electrochemical sensors, molecularly imprinted sensors, paper-based biosensors, microfluidic (lab-on-a-chip) assays, chemiresistive and field effect transistor–based sensors, and giant magnetoresistive sensors. Tables are presented that give an overview on the wealth of methods and materials. A concluding section summarizes the current status, addresses current challenges, and gives an outlook on potential future trends.

Keywords Biomarkers · CA125 · MUC1 · Prostasin · HE4 · Nanosensors · Flexible FET, electrochemical · Molecular imprinting · Microfluidic

Introduction to ovarian cancer

Ovarian cancer is known as a fatal gynecologic cancer. It is not a distinct malignancy and consists of epithelial and non-epithelial kinds with subclasses of epithelial ovarian cancer depending upon grouping of structural and medical topographies [1]. Because of poor diagnosis, the identification of key factors for the prevention of ovarian cancer may have significant medical and public health implications. The stage of ovarian cancer during diagnosis plays a vital role that can be divided into various stages, viz., stages I, II, III, and IV. In stage I, cancer is totally confined to only ovary, while in later stages, it spreads outside the pelvis to other portions of the body through metastasis. Metastases occur either via lymphatics to nodes at the renal hilus or via blood vessels to the parenchyma of the liver or lung. Most often, lesser masses of cancer cells are shed by the ovary and embed on the surface of peritoneal, thus making several nodules. In case of ovarian cancer, contrasting to other cancers, no anatomical hindrance is present to widespread metastasis during the course of the peritoneal cavity. Tumor grafts block lymphatic vessels that pass through the diaphragm, thereby inhibiting the discharge of ascites fluid which outflows from the disordered tumor vessels in the presence of high levels of tumor-derived vascular endothelial growth factor A (VEGFA), which is known as a vascular permeability factor. Antibodies that deactivate VEGFA have lessened the buildup of ascites in animal models and in medical studies [2–4].

Ovarian cancer at initial stage normally exhibits very few exact symptoms. Thus, the 5-year survival level among more than 70% patients in advanced stage of diagnosis is less than 30%. If it is properly identified in stage I, ~ 90% of patients can be cured with the help of standard surgery and chemotherapy. But, only 25% are diagnosed in stage I because of the nonappearance of specific early warning signs [5]. When

Electronic supplementary material The online version of this article (https://doi.org/10.1007/s00604-020-4152-8) contains supplementary material, which is available to authorized users.

✉ Sushmee Badhulika
sbadh@iith.ac.in

[1] Department of Electrical Engineering, Indian Institute of Technology, Hyderabad 502285, India

ovarian cancer is detected in advanced stage, the survival rate of patients is very poor, only 10–30% [6, 7].

Even though there are various precautionary methods being practiced globally, the overall ovarian cancer mortality rate is on the rise which is because of increasing obesity among populations and usage of the oral contraceptive pills. Therefore, there is an extreme necessity to identify it in early phases. There are several approaches used for its identification, mainly focusing on the presence of ascites followed by pelvic test to check the size of an ovary. Nonetheless, these techniques are expensive and laboratory-based and need time-consuming step-based analysis and skilled technicians. To address these issues, it is important to develop new and miniaturized sensing methodologies that would help the ovarian cancer–affected patients to get screened early and with ease. In this regard, the use of sensitive biosensors for recognition and continuous monitoring of ovarian cancer would be an excellent alternative.

A diversity of nanomaterials of various structures, chemical compositions with desirable surface properties, crystallographic orientations etc. had led to their widespread use in energy, biosensing applications [8–13]. The ability to tailor the structure and therefore the properties of nanomaterials provide brilliant projections towards fabrication of the novel biosensors and improve their performances. Biosensors can be categorized into various groups based on the mode of signal transduction. The objective of this review is to highlight current advancements in fabrication of different types of nanomaterial-based biosensors for ovarian cancer diagnosis. Thus, this review comprises of a brief overview of previously reported optical, electrical, electrochemical, micro-fluidic, paper-based, or flexible biosensing platforms towards determination of several ovarian cancer biomarkers.

Biomarkers for ovarian cancer

Biomarkers are the biomolecules which act as an index of a specific biological process or disease. Continuously monitoring the level of any biomarker in a particular biological media that could be serum, plasma, cellular fluid etc., often is critical in medical diagnosis. In this section, we briefly discuss about ovarian cancer–specific biomarkers.

Cancer antigen CA125 (MUC16)

CA125 (mucin 16), an important biomarker for checking the diagnosis, evolution, and management of ovarian cancer, is produced by the mesothelial cells and epithelial ovarian tumors. It is encoded by MUC16 gene and articulated as a protein of membrane bound at cells' surface that carry out metaplastic differentiation into a Mullerian-type epithelium or released in biological fluids in solvable form. The standard level of CA125 in human blood is typically < 35 units per milliliter (U mL^{-1}), and beyond this level, it would cause the progression of ovarian cancer [14–16].

Human epididymis protein 4

Human epididymis protein 4 (HE4) is a vital biomarker for early identification of ovarian cancer and is also considered a primary sign of disease recurrence. It is firstly recognized in the epithelium of the distal epididymis and predicted to be a protease inhibitor involved in sperm maturation [17–20]. Nevertheless, the utilization of CA125 as a biomarker for initial recognition of ovarian cancer is strictly limited as its concentration is raised in only half of early-stage ovarian cancers and often in several benign gynecological diseases including ovarian cysts, endometriosis, and pelvic inflammation [20, 21]. Henceforth, quantification of HE4 with very low concentration in combination with CA125 is of prime significance and thus providing the paramount technique of differential diagnosis in ovarian cancer and other genital masses [22–24].

Prostasin

Prostasin is generated at higher level in epithelial ovarian cancer and should be examined more as a biomarker either alone or in combination with CA125. As per our knowledge, very few reports on nanomaterial-based biosensors for recognition of this biomarker have not been published [16].

Mucin 1

Mucin 1 (MUC1), glycoprotein encoded by the MUC1 gene is articulated with high concentrations in all epithelial cell adenocarcinomas for the breast and ovarian cancer patients. The increasing expression of MUC1 results in large amounts of free protein found in the blood [25]. Thus, determination of MUC1 is of excessive significance in cancer identification.

Conventional diagnostic methods for diagnosis of ovarian cancer

Conventional diagnostic methods like mass spectrometry [26, 27], immunoassay [28], radioimmunoassay [29], enzyme-linked immunosorbent assay (ELISA) [30, 31], and polymerase chain reaction (PCR) [32, 33] have been used for biomarker determination. But these techniques involve intricate sample pre-treatment, necessity of employing professional personnel, expensive, sophisticated instrumentation, long data analysis time, cautious washing, and separation stages. Henceforth, it is essential to fabricate cost-effective, sensitive sensors with quick response time.

Biosensors for determination of ovarian cancer

Biosensing has major scientific significance in betterment of human life in terms of disease identification and treatment [34, 35]. This has directed the scientists to emphasis on developing simple biosensors with excellent analytical performances. A biosensor is a diagnostic device that translates the information about the existence of a chemical species (analyte) to an assessable indication. It comprises 2 main constituents: (a) receptor and (b) transducer. The receptor is a biomolecule, that distinguishes the analyte, and the transducer translates this determination incident into a useful signal like current, magnetoresistance, and absorbance. Widely used biorecognition elements are enzyme, antigen (Ag), antibody (Ab), or oligonucleotide [35, 36]. Immunosensors, one of the most significant classes of biosensors, have been broadly employed to sense protein biomarkers depending on Ag–Ab interaction with extraordinary sensitivity and particularly brilliant selectivity. It can be classified further into two types: (a) labeled and (b) label-free immunosensor. In label-free immunosensor, the target molecules are directly quantified from the antigen/antibody interaction wherein the labeled immunosensors employ a label or tag as well as an additional secondary Ab, namely, Ab_2, to amplify the signal in addition to primary Ab, named Ab_1 [37, 38].

Optical biosensors

Fluorescence-based biosensors

Jin et al. [39] demonstrated the photoluminescence (PL)-based biosensors using the aptamer (one class of artificial oligonucleotides) and 5-fluorouracil (5-Fu)-loaded Ag_2S quantum dots (QDs). The surface of QDs was decorated with polyethylenimine, followed by combination with the aptamer/5-Fu complex to make Ag_2S QDs/aptamer/5-Fu composite. In amalgamation of Ag_2S QDs with aptamer/5-Fu complex, near-infrared (NIR) PL of QDs was reduced, ascribed to photo-induced electron transfer from QDs to 5-Fu (Fig. 1a(i)). The adding of CA125 made a recognizable NIR PL recovery. Hence, this composite was established as NIR PL turn-on probe for CA125, exhibiting a limit of detection of 0.07 ng mL^{-1} over the linear range of 0.1 to 10^6 ng mL^{-1} with high sensitivity and selectivity and a good corelation coefficient (R^2) of 0.9961 (Fig. 1a(ii)). The practicability of this NIR PL probe for CA125 recognition was assessed by inspecting its performance in human serum, urine, and gastric juice.

Fluorescence resonance energy transfer (FRET) depends on the energy transfer between two fluorescent molecules, i.e., donor and acceptor [41, 42]. Hamd-Ghadareh et al. [43] developed FRET immunosensing of CA125 employing the carbon dots (CDs). The CDs functionalized with aptamer were used as a recognition probe wherein polyamidoamine (PAMAM)–dendrimers/gold nanoparticle (NP) composite was utilized for covalent attachment of CA125-Ab. This immunosensor displayed a limit of detection (0.5 fg mL^{-1}) over the linear region of 1.0 fg mL^{-1}–1.0 ng mL^{-1} of CA125 with good selectivity and sensitivity. This assay is suitable for the recognition of OVCAR-3 cancer cells in the region of 2500–20,000 cells with detection limit 4 cells/10 μL along with selective imaging of the cancer cells. Wang et al. [25] demonstrated the gold NP–CD composite as a fluorometric assay towards determination of MUC1 that showed good linearity over the MUC1 concentration range of 5.3–200 ng mL^{-1}, a high detection limit of 5.3 ng mL^{-1} and good selectivity. But, salt was used for recovering the fluorescence of the CDs during sensing. Ma et al. [44] presented the fluorescence assay for MUC1 based on the aggregation of CDs with a size of ~2 nm that showed strong blue-green intrinsic fluorescence. MUC1 Abs and the MUC1 aptamer were covalently attached with the CDs. The sensing was performed through plotting the changes in fluorescence with the MUC1 concentrations over the range of 5–100 nM with a detection limit of 2 nM. The assay was also used to determine MUC1 in serum samples. But the synthesis procedure of the CDs was time-consuming, multiple step–based, and using acid-like concentrated sulfuric acid. Yang et al. [45] used a rolling mediated cascade amplification strategy to improve the visualization of MUC1 profiling on cell surfaces where the CdTe QDs were used as fluorescent labels. Li et al. [46] demonstrated a fluorometric assay for MUC1 based on signal amplification of the hybridization chain reaction, and the interaction between a luminescent ruthenium (II) complex and CdZnTeS QDs. This sensor exhibited a very low detection limit of 0.13 ng mL^{-1} in MUC1 concentration range of 0.2–100 ng mL^{-1}. The method was also applied towards determination of MUC1 in spiked serum samples.

Surface plasmon resonance

Surface plasmon resonance (SPR) sensors employ surface plasmon waves to delineate alterations during interaction between the target molecule and bioreceptor on the sensor and they are sensitive towards the refractive-index change of their surrounding media [47, 48]. Suwansa-ard et al. [49] reported a N-ethyl-N0-(3dimethyl-amino-propyl-carbodiimide (EDC)-N-hydroxysuccinimide (NHS) functionalized gold surface-based SPR sensor for determination of CA125 where anti-CA125 was immobilized on gold surface using a self-assembled monolayer (SAM). The sensor showed detection limit of 0.1 U mL^{-1} over a narrow linear region of 0.1–40 U mL^{-1} that makes them not suitable for practical applications. Zhang et al. [50] presented a SPR sensor using gold nanorods. The concentrations of CA125 were determined by examining the level of gold nanorods' aggregation triggered by CA125 Ab–Ag interactions. This sensor was able to detect 0.4 U mL^{-1} of CA125 over the linear region of 1–80 U mL^{-1} with good reproducibility. Yuan et al.

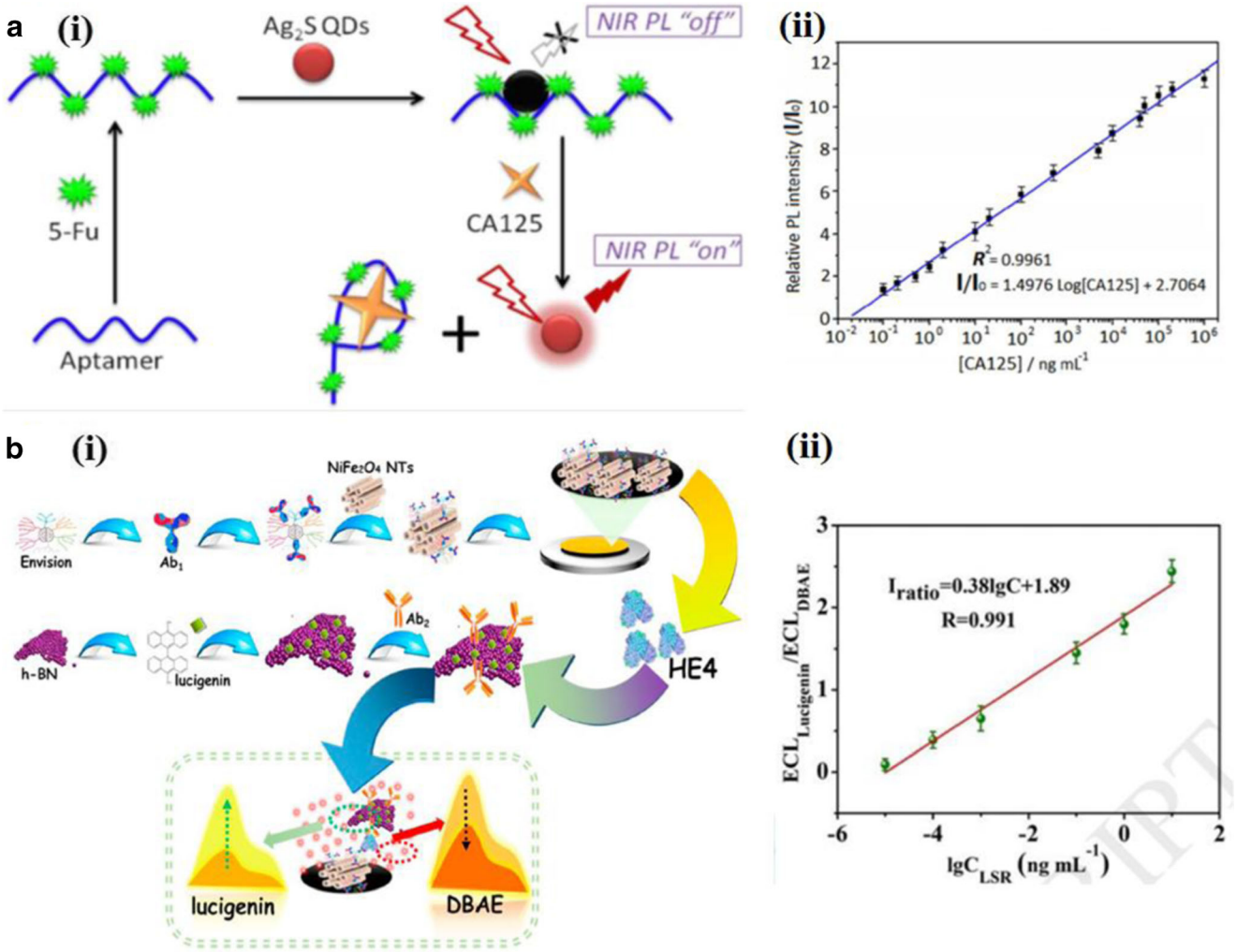

Fig. 1 **a** (i) Graphical representation of the fabrication routes of NIR PL sensor; (ii) corresponding calibration plot. Reprinted with the permission from [39]. **b** (i) Schematic depiction of the fabrication steps of the ECL-based HE4 immunosensor; (ii) calibration plot. Reprinted with the permission from [40]

[51] used silver (Ag) nanochip-based localized SPR (LSPR) sensor towards determination of HE4 where the nanochip was incubated in 11-mercaptoundecanoic acid solution to produce SAM on its surface, followed by activation of this layer with EDC-NHS. Afterwards, anti-HE4 solution was immobilized on the electrode's surface and the HE4 was subjected for final LSPR measurements. The quantifiable recognition of HE4 was done by observing the $\Delta\lambda_{max}$ when the target HE4 molecules were bound to the NPs. This sensor showed low detection limit of 4 pM, decent selectivity, reproducibility, and durability over the linear range of 10–10,000 pM. The good correlation between LSPR and ELISA results in human serum ensures its suitability for real-time applications.

Chemiluminescence-based optical biosensors

Chemiluminescence (CL) employs energy resulting from chemical reaction that yields a luminescence emission of light because of the relaxation of the atoms from excited state to ground state. The reaction between the immobilized biomolecule marked with CL species and analyte results in generating light owing to this reaction [47]. Yang et al. [52] developed the 3D silica film for CL sensing of CA125 where the sensor displayed a wide range of 0.5–400 U mL^{-1} with good reproducibility and durability. In applicability tests with the serum samples, the relative errors were high (~ 8%). Al-Ogaidi et al. [53] used graphene QDs for recognition of CA125 which showed low limit of detection limit (0.05 U mL^{-1}) over the linear range of 0.1–600 U mL^{-1}. It is a well-substitute for a FRET-based assay as it removes the requirement of an additional excitation source.

Electrochemiluminescence-based optical biosensors

Electrochemiluminescence (ECL) is defined as a chemiluminescence activated by electrochemical method. Upon ECL

reaction, the emitted light is identified in present of a required voltage [8]. Wang et al. [40] presented nickel–iron oxide ($NiFe_2O_4$) NT-based electrochemiluminescent sensor for determination of HE4. A polymeric material enhanced the ECL emission method of 2 luminophors via decomposition of hydrogen peroxide (H_2O_2). The hexagonal boron nitride nanosheets immobilized large amount of lucigenin, thereby retaining stable ECL emission of lucigenin (Fig. 1b(i)). It exhibited low detection limit of 3.3 fg mL^{-1} over the linear range of 10 fg mL^{-1}–10 ng mL^{-1} of HE4 as illustrated in Fig. 1b(ii). Acceptably, the relative standard deviation (RSD) of DBAE and lucigenin were 0.18% and 0.48%, respectively, indicating its good stability. Babamiri et al. [54] used the PAMAM-QDs and PAMAM-sulfanilic acid-$Ru(bpy)_3^{2+}$ for CA125 sensing where the CdTe/CdS QDs and $Ru(bpy)_3^{2+}$ in presence of tripropylamine were acted as co-reactant for generation of ECL and Fe_3O_4–SiO_2 was employed as a magnetic bead. This sensor showed low limit of detection (0.1 μU mL^{-1}) over the linear region of 1 μU mL^{-1}–1 U^{-1} of CA125. The results obtained with this immunosensor agree well with the results of ELISA as reference method, thus confirming its suitability towards practical applications. Tan et al. [55] described an ECL immunoassay for CA125 determination utilizing CdSe nanocrystals. This sensor displayed the limit of detection of 5×10^{-5} U mL^{-1} over the linear region of 10^{-4}–1 U mL^{-1}. Wu et al. [56] demonstrated an ECL sensor constructed on graphitic carbon nitride (g-C_3N_4)–based electrode for CA125 recognition. This sensor revealed a widespread linear range for CA125 (0.001–5 U mL^{-1}) and limit of detection (0.4 mU mL^{-1}). But its narrow detection range might not be suitable for the practical applications.

A summary of the reported methods, the importance of nanomaterials, and the recognition procedures utilized in optical sensing of ovarian cancer biomarkers is summarized in Table 1.

Electrochemical biosensors

The electrochemical determination techniques have been found promising in biosensing applications because of various benefits including high sensitivity, specificity, low cost, low detection limit, good reliability, and easiness in handling [37, 57–62].

Raghav et al. [63] developed gold–Ag NP–based label-free detection of CA125. Direct immobilization of Ab on the surface of the electrode exhibited good linear response over 1–150 IU mL^{-1} ($R^2 = 0.994$) and tolerable interference. This immunosensor showed sensitivity of 190 Ω IU^{-1} mL cm^{-2} which was because of high specific surface area for their core–shell structure. This immunosensor exhibited acceptable interference of 2–5% from serum components and retained 90% stability up to 20 days, thus displaying its suitability towards practical applications. Wang et al. [64] reported the TbFe-based combined metal–organic frameworks (MOF) to detect CA125 that showed a limit of detection of 58 μU mL^{-1} over a linear region of 100 μU mL^{-1}–200 U mL^{-1} with excellent selectivity and stability, satisfactory reproducibility, and good applicability in serum. Johari-Ahar et al. [65] demonstrated an immunosensor for CA125 sensing where gold electrode was modified with mercaptopropionic acid and successively then conjugated with silica (SiO_2)-coated gold NPs, CdSe QDs, and CA125 monoclonal antibody (mAb) (Fig. S1). The nanobiosensor displayed high stability and reproducibility and an ultra-low limit of detection (0.0016 U mL^{-1}) over the region of 0–0.1 U mL^{-1}. The applicability of the immunosensor was inspected by assessing CA125 concentration in the serum collected from the ovarian cancer patients.

Torati et al. [66] presented gold-based label free immunosensor towards CA125 recognition. The electrode was amine functionalized using cysteamine hydrochloride followed by activation with EDC-NHS. This immunosensor displayed linearity over narrow region ranging from 10 to 100 U mL^{-1} with high limit of detection of 5.5 U mL^{-1}, thereby making it unsuitable for real-time applications. Zheng et al. [67] used the label-free Prussian Blue-Platinum (Pt)-NP-polyaniline composite–based bio-electrode for CA125 sensing which exhibited good linearity over the concentration range of 0.01–5000 U mL^{-1} and detection limit of 4.4 mU mL^{-1} with a sensitivity of 119.76 μA·$(U/mL)^{-1}$ cm^{-2}. Gasparotto et al. [68] fabricated the gold NP-zinc-oxide (ZnO)-based nanohybrid for label-free CA125 determination and displayed a limit of detection (2.5 ng $μL^{-1}$) with high reproducibility, specificity, and notable durability. Gazze et al. [69] established a graphene–polyaniline-based biosensor for label-free recognition of CA125, and this electrode was then functionalized with anti-CA125 Ab by covalent cross-linking to polyaniline. This was able to detect CA125 as low as concentration of 0.923 ng $μL^{-1}$ over the linear range of 0.92 pg $μL^{-1}$–15.20 ng $μL^{-1}$. Ravalli et al. [70] used the gold NP–modified electrode for label-free recognition of CA125 where the immunoassay was founded on SAM of gold NP–based electrodes followed by immobilization of monoclonal Ab anti-CA125. This sensing layer was also activated with EDC-NHS and able to detect CA125 concentrations in the range of 0–100 U mL^{-1} with high detection limit of 6.7 U mL^{-1}. Jafari et al. [71] presented the Ag NP–graphene quantum dot (GQD) composite-modified label-free electrode which was able to detect 0.01 U mL^{-1} of CA125. Ren et al. [72] reported the ferrocenecarboxylic acid (FA), HCl-doped polyaniline, and chitosan hydrochloride composite as a substrate material for producing signal and enlarging specific surface area, and Ag–Co_3O_4 nanosheets were employed in this immunosensor for intensifying the antibody capacity. This biosensor showed detection limit of 0.25 pg mL^{-1} over the concentration range of 0.001–25 ng mL^{-1} with acceptable stability and reproducibility. Its good recovery percentage in the serum samples ensures suitability of this sensor in the clinical diagnosis.

Table 1 List of nanomaterial-based optical biosensors towards determination of ovarian cancer biomarkers

Ovarian cancer biomarkers	Nanomaterials	Recognition methods	Detection limit	Linear range
CA125	Ag_2S QDs	PL	0.07 ng mL^{-1}	0.1–10^6 ng mL^{-1} [39]
CA125	CDs	FRET	0.5 fg mL^{-1}	1 fg mL^{-1}–1 ng mL^{-1} [43]
MUC1	Gold NP–CD composite	Fluorescence	5.3 ng mL^{-1}	5.3–200 ng mL^{-1} [25]
MUC1	CDs	Fluorescence	2 nM	5–100 nM [44]
MUC1	Ruthenium (II) complex–CdZnTeS QDs	Fluorescence	0.13 ng mL^{-1}	0.2–100 ng mL^{-1} [46]
CA125	Gold	SPR	0.1 U mL^{-1}	0.1–40 U mL^{-1} [49]
CA125	Gold nanorods	SPR	0.4 U mL^{-1}	1–80 U mL^{-1} [50]
HE4	Ag nanochip	SPR	4 pM	10–10,000 pM [51]
CA125	3D-ordered nanoporous silica	CL	-	0.5–400 U mL^{-1} [52]
CA125	Graphene QDs	CL	0.05 U mL^{-1}	0.1–600 U mL^{-1} [53]
HE4	$NiFe_2O_4$ nanotubes	ECL	3.3 fg mL^{-1}	10 fg mL^{-1}–10 ng mL^{-1} [40]
CA125	PAMAM-QDs and PAMAM-sulfanilic acid-$Ru(bpy)_3^{2+}$	ECL	0.1 μU mL^{-1}	1 μU mL^{-1}–1 U^{-1} [54]
CA125	CdSe nanocrystals	ECL	5×10^{-5} U mL^{-1}	10^{-4}–1 U mL^{-1} [55]
CA125	g-C_3N_4	ECL	0.4 mU mL^{-1}	0.001–5 U mL^{-1} [56]

Pakchin et al. [73] reported the chitosan–gold NP–CNT–graphene oxide (GO) composite-based bio-electrode and lactate oxidase (Lox) as a label towards CA125 sensing. When a target Ag is linked with an associated Ab, a secondary Ab is used as label to generate the indication. To attain an extremely sensitive sandwich kind of immunosensor, a greater number of Abs on the electrode's surface and label is essential. To increase the functional groups, chitosan, a highly abundant biopolymer with inherent functional groups on its surface, was utilized. But, it suffers from poor conductivity. To enhance direct electron transfer rate, the gold NP–CNT–GO composite was used for sensing along with chitosan. Figure S2 illustrates the graphical representation of fabrication stages of the immunosensor. The sensing performance was studied in terms of the H_2O_2 oxidation that presented low limit of detection (0.002 U mL^{-1}) with excellent reproducibility, selectivity, and durability towards CA125 determination. The recovery results and its comparison of this immunosensor by the ELISA method confirmed its applicability for the real biological sample analysis with good accuracy and reliability. Taleat et al. [74] used a sandwich format based on polyanthranilic acid-based electrode. This sandwich assay was then achieved through addition of anti-CA125 Ab_2 labeled with gold NPs. The antibody-gold NPs captured onto the bioelectrode surface induced the deposition of Ag from its precursor solution. With the increasing concentration of CA125, more numbers of gold NPs were captured on the surface of the immunoelectrode to generate more numbers of Ag NPs. Over a narrow region of 5–25 U mL^{-1}, the biosensor was able to detect 2 U mL^{-1} of CA125 with satisfactory sensitivity, selectivity, and reproducibility. Liang et al. [75] developed a sandwich-typed sensor based on pH reactive sensitivity amplifiable method for CA125 sensing. Firstly, the pH responsive polydopamine framework was prepared using zeolitic imidazolate framework as a template. This polydopamine–methylene blue composite was then covalently attached with Ab_2 and utilized as a label. The gold-reduced graphene oxide (rGO) composite was functioned as substrate to capture target molecules, HCl was used for the annihilation of label and disassociation of Ag–Ab interaction layer, thus decreasing the impedance and enhancing the electron transfer efficacy. This immunosensor revealed a low limit of detection (0.336 μU mL^{-1}) with acceptable reproducibility, sensitivity, and selectivity over the linear region of 0.0001–100 U mL^{-1}. Wu et al. [76] reported the gold NPs and horseradish peroxidase (HRP) was used as a label. The current was decreased with the increasing concentrations of CA125 ranging from 0 to 30 U mL^{-1} with high limit of detection (1.73 U mL^{-1}) with acceptable stability. A reduction of 10.3% in amperometric response in human serum after a 7-day storage confirms its incompatibility for routine clinical diagnosis.

Wu et al. [77] developed a carbon nanofiber for binding of CA125 and thionine was used as electron transfer mediator. The carbon nanofiber was activated and functionalized with EDC-NHS and HRP was employed as a label (Fig. S3). The labeled conjugate revealed a decent enzymatic activity towards electro-oxidation of thionine by H_2O_2. This sensor displayed satisfactory sensitivity, stability, reproducibility, and limit of detection of 1.8 U mL^{-1}. Lu et al. [78] reported a labeled, gold NP–chitosan–titanium carbide (TiC)–based immunosensor for determination of HE4. The Ab_1 namely, anti-HE4, was immobilized on the electrode surface. After immunoreaction, HE4, Ab_2, and primer DNA were immobilized on the Ab_2. This sensor exhibited low limit of detection (0.06 pM) over a linear concentration range of 3–300 pM of HE4 with good precision and regenerative ability.

Paimard et al. [79] presented an impedimetric assay for MUC1 using the core–shell nanofiber-multi-walled carbon nanotube (MWCNTs)–gold NP composite which was covalently modified with the MUC1-binding aptamer. MUC1 was sensed through the change of the resistance of the electrode surface. This sensor exhibited a high detection limit (2.7 nM) and good stability and selectivity over the narrow region of 5–115 nM of MUC1. The assay was successfully applied towards MUC1 determination in spiked serum samples with satisfactory recovery. Guo et al. [80] demonstrated the Ag nanocluster–based electrode for MUC1 sensing. This sensor exhibited a low detection limit of 0.5 nM over the wide MUC-1 concentration ranging from 1 to 500 nM. But they used the template (C_{12}) during preparation of Ag nanoclusters.

Molecular imprinting technique

Molecular imprinting is a technique to generate precise active sites with high affinity towards target molecule in polymers via molecular template. Molecularly imprinted polymers (MIPs), also known as cross-linked polymers, are tailor-made materials. Three-dimensional cavities are produced inside polymer corresponding to the shape and size of the target molecule. The imprinted polymer cavities permit the target molecules to reside in the cavity space. Target molecules can also be utilized as a template for imprinting polymers. MIPs can be made easily and are stable, and unaffected to an extensive range of pH, temperature, and solvents. Deposition of MIPs on the surface of nanostructure-modified electrodes increases sensitivity for biomolecule sensing [81, 82].

Viswanathan et al. [83] presented the protein-imprinted polymer on 3D gold nanoelectrode for CA125 quantification wherein CA125 was firstly used as a template and upon its removal imprints for CA125 (Fig. 2a). The protein-imprinted sites on nanoelectrode are then employed for immunospecific internment of CA125 molecules, and the mass of bound on the electrode surface was noticed as a drop in the faradic current from the redox indicator. The sensor displayed decent linearity over the concentrations ranging from 0.5 to 400 U mL^{-1} with high limit of detection (0.5 U mL^{-1}) (Fig. 2b). Replicated 5 independent analyses were directed to RSD of 3.1% only. In human serum samples, the recovery outcomes and its comparison of this immunosensor by the ELISA method confirmed its suitability for the real biological sample analysis.

Büyüktiryaki et al. [84] testified the phosphoserine (PS)-imprinted CNT–Fe_2O_3 NP-polymer-based nanosensor for CA125 quantification where methacryloyl antipyrine europium(III) [$(MAAP)_2$–Eu(III)] and methacryloyl antipyrine terbium (III) [$(MAAP)_2$–Tb(III)] were utilized as monomers and PS was employed as template. This MIP sensor was able to detect 0.49 U mL^{-1} of CA125 with good sensitivity and reproducibility.

Paper-based biosensors

Paper-based biosensors have attracted significant interest because of their several benefits like inexpensiveness, disposability, biocompatibility, and abundance. Various approaches like UV photolithography, wax printing, and screen printing have been developed for the fabrication of paper-based biosensors [85–87].

Fan et al. [88] demonstrated the rGO–thionine–gold NP–modified paper-based immunosensor towards CA125 determination (Fig. S4**)**. CA125 was detected through the reduction in the values of current upon binding of CA125 Ab and Ag. The paper-based immunosensor exhibited low limit of detection (0.01 U mL^{-1}) over the linear region of 0.1–200 U mL^{-1} with great accuracy, reliability, reproducibility, and stability. In serum samples, the relative error was high nearly ~ 8.05%. Ge et al. [89] developed an array of addressable, chitosan–MWCNT composite-modified paper electrodes which were assembled on the crossing points of the row/column electrodes using a device holder used for quantification of CA125. One paper layer comprised of the sensing sites, the other paper layers for the printed counter electrode, and reference electrode. This sensor displayed low limit of detection (3.7×10^{-5} U mL^{-1}) with outstanding linearity, durability, and reproducibility over the linear range of 1×10^{-4}–100 U mL^{-1}.

Bahavarnia et al. [90] fabricated a paper-based biosensor through hand writing of Ag/rGO nanoink on paper towards recognition of CA125 in human biofluid. Paper electrode was modified by cysteamine (CysA)-caped gold NPs and from the amine group with hydroxyl and carboxyl groups of Ag/rGO nanoink deposited on the surface of paper-based electrode. Then, anti-CA125 was immobilized on the electrode surface via gold NPs and CA125 interaction. The sensor displayed low limit of detection (0.78 U mL^{-1}) over the region of 0.78–400 U mL^{-1} with poor stability.

Microfluidic-based lab-on-chip devices

Microfluidic-based lab-on-chip biosensor is one of the powerful miniaturized devices that eases the incorporation of manifold functionalities of one or more sensing platforms on a single system, consuming less sample volume. Microfluidic devices facilitate effective recognition of biomolecules at the expense of small volume of reagents and energy, thus paving a new avenue towards development of the point-of-care (POC) devices [91].

Mandal et al. [92] developed a microfluidic, capacitive, carboxyl CNT–based biosensor for determination of CA125 which was successfully incorporated with polydimethylsiloxane (PDMS) microfluidic channels. Only 5 μL of CA125 Ag solution was employed on the channel inlet. The Ag solution was then passed through this channel because of capillary effect and interacted with Ab that was exposed on top of the

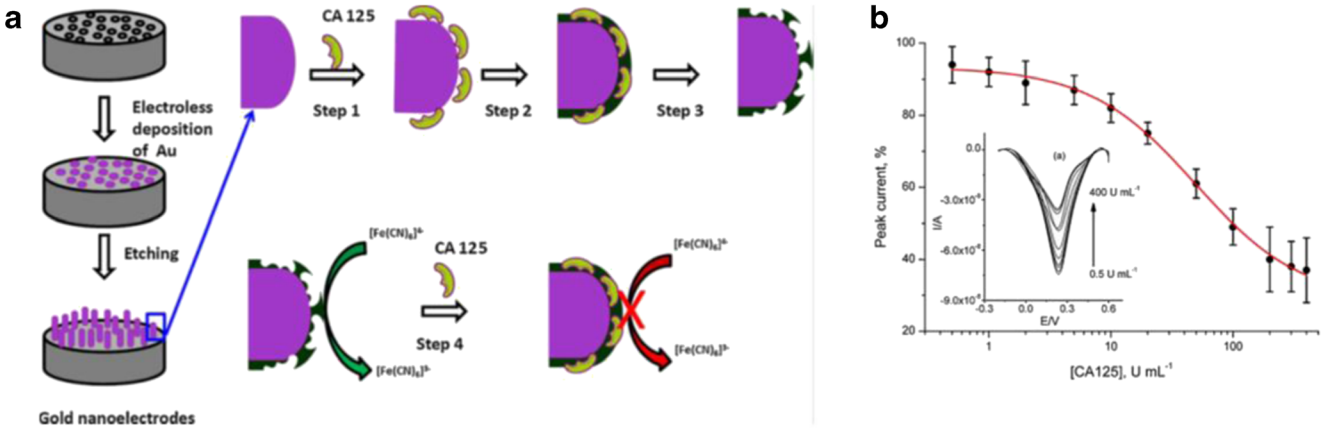

Fig. 2 **a** Schematic depiction of MI protein sensor. Step1: adsorption of CA125 on the electrodes' surface. Step 2: electro-polymerization of phenol. Step 3: removal of template protein. Step 4: CA125 binding and signal generation. **b** Corresponding calibration plot. Inset of (**b**) is as follows: DPV results to CA 125. Reprinted with the permission from [83]

sensing device (Fig. 3a, b). The experiments were performed in two cases, (a) only phosphate-buffered saline (PBS) was passed through the microchannel and corresponding capacitive curve was considered "baseline" and (b) the capacitive measurements were executed while CA125 Ag solution was passed through. The Ag–Ab interaction yielded the change in the medium's dielectric properties over the sensor surface. Ag–Ab conjugation capacitance of the carboxylic CNT-based microfluidic base device was higher than non-carboxylic CNT- and non-CNT-based biosensors (Fig. 3c) as unavailability of covalent attachment of the CNTs between CA125 Ab and SAM caused a loss of both CNTs and Ab underneath the shear flow state, thus providing less number of Ab present for the Ag–Ab conjugation and lowering the net capacitance. As the CNTs and Ab have higher dielectric permittivity, this microfluidic sensor exhibited remarkably greater capacitance than the non-CNT-based sensor.

Wang et al. [93] used a labeled, 3D microfluidic immunodevice for the determination of CA125. Molybdenum disulfide (MoS_2) was acted as support for CA125 (Ab_1) wherein the gold nanoflowers were used as the supporter of glucose, glucose oxidase (GO_x), and CA125 secondary Ab (Ab_2). The microfluidic system was made up using screen-printed electrodes on wax-patterned cellulose paper. GO_x catalyzed glucose oxidation while MoS_2 enhanced the reduction of H_2O_2. The immunosensor revealed great sensitivity, specificity, and low detection limit of 0.36 pg mL^{-1} with excellent linearity over the CA125 concentration range of 0.001–50 ng mL^{-1}. This work paved a unique route towards the fabrication of POC devices founded on microfluidic paper-based analytical devices (μ-PADs). Wu et al. [94] presented the combination of polymerization-aided signal amplification with μ-PAD wherein the μ-PAD was fabricated using the photoresist-patterning as well as screen-printing methods. Glycidyl methacrylate was polymerized to offer epoxy groups for immobilization of label, HRP on the surface of GO–chitosan-modified paper electrode. CA125 was detected using the HRP-O-phenylenediamine-H_2O_2 electrochemical system which showed 0.05 ng mL^{-1} with good reproducibility, stability, and regeneration. The practicability was not shown. Nunna et al. [95] reported the gold NP–modified microfluidic biosensor for CA125 determination. The capacitive response of Ag–Ab conjugation on inter-digitated electrodes was boosted up by ~2.8-fold in static drop state and ~2.5-fold in microfluidic flow state with gold NP modification. Zhao et al. [96] demonstrated a microfluidic ExoSearch chip for multiplexed exosome recognition towards CA125 sensing that offers a continuous-flow strategy for quantifiable segregation and liberation of blood plasma exosomes in large range of preparation volumes (10 μL–10 mL) with good reproducibility (coefficient of variation, CV < 10%).

Chemiresistive or field effect transistor–based biosensors

Recognition of various target biomolecules using chemiresistive or field effect transistor (FET)–based sensors have gained wide attention among research communities as they involve a nominal or no sample preparation and make suitable for on-site monitoring because of quicker transduction mechanism. The transportability and entire analytical performances of the sensors can be enhanced by using nanostructures as attractive channel materials. Owing to small cross-sectional area, the nanostructures display no horizontal current shunting, thereby exhibiting excellent response.

Majd et al. [97] developed the flexible FET-type aptasensor for CA125 determination based on carboxylated MWCNT–rGO composite wherein poly(methyl methacrylate) (PMMA) was utilized as a substrate. RF sputtering method was used to deposit the source/drain gold electrodes while Pt was employed as gate electrode. A solution chamber containing 20 μL was employed for the measurements. The carboxylated MWCNTs were activated with EDC-NHS followed by

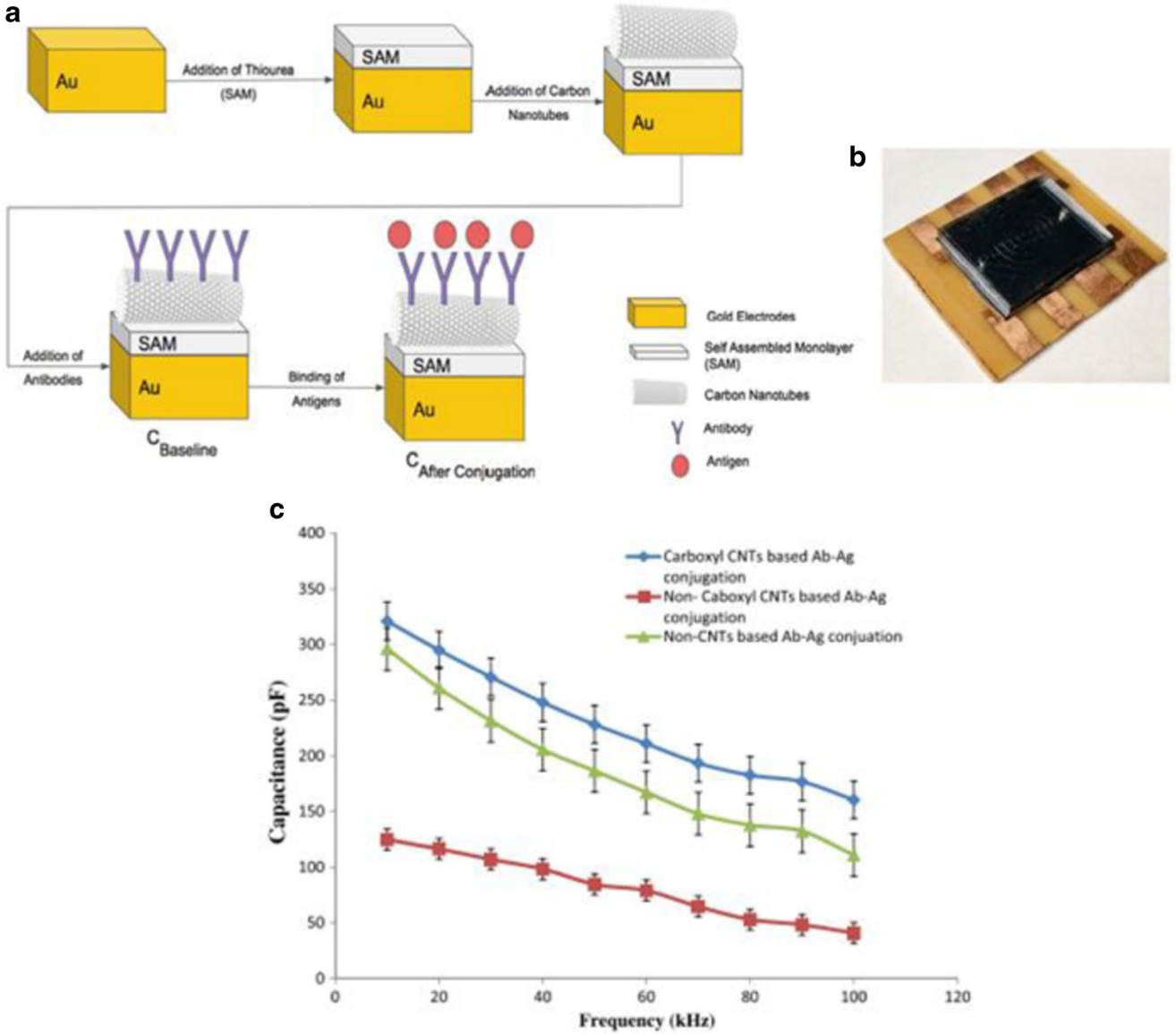

Fig. 3 **a**, **b** Schematic diagram of microfluidic, carboxyl CNT–based sensor for CA125 recognition. **c** Comparison in the capacitive performances of the carboxyl CNTs and non-carboxyl CNTs and non-CNT-based biosensor. Reprinted with the permission from [92]

immobilization of CA125 single strand DNA (ssDNA). The rGO surface was then modified with incubation of MWCNT-CA125 aptamer through π–π interaction. In the I–V curves (Fig. 4a), after deposition of MWCNTs modified with CA125 ssDNA on rGO channel, dI/dV increased significantly as MWCNTs with great specific surface area reduced the electrode resistivity whereas dI/dV decreased upon CA125 incubation. Figure 4 b illustrates the flexible liquid-ion-gated FET-based nanobiosensor. Under the gate voltages (Vg) ranging from − 1 to + 1 V at a fixed drain voltage (Vd = 0.2 V) in rGO FET (Fig. 4c), the drain current (Id) increased with the increasing Vg, signifying n-type characteristics. Figure 4 d displayed the transfer characteristics of the rGO FET nanosensor before and after incubation of 1.0×10^{-5} U mL^{-1} CA125. The current values of the rGO/MWCNTs/CA125 ssDNA aptasensor decreased because of interaction of CA125 ssDNA-wrapped MWCNTs with graphene and phosphate groups of the ssDNA are negatively charged gates, thus decreasing the current of the n-type channel. This aptasensor showed a good linear range for CA125 (1.0×10^{-9}–1.0 U mL^{-1}), a low limit of detection (5.0×10^{-10} U mL^{-1}) with selectivity, stability, and flexibility as exhibited in Fig. 4e. The reproducibility of this FET biosensor was also evaluated through conducting experiments for 1×10^{-5} U/mL of CA125, and it revealed the response with RSD 3%. Good agreement between the ELISA method and this aptasensor ensures its applicability towards the determination of CA125 in real human serum samples.

Bangar et al. [98] demonstrated the polypyrrole (Ppy)-based chemiresistive immunosensor for CA125 determination.

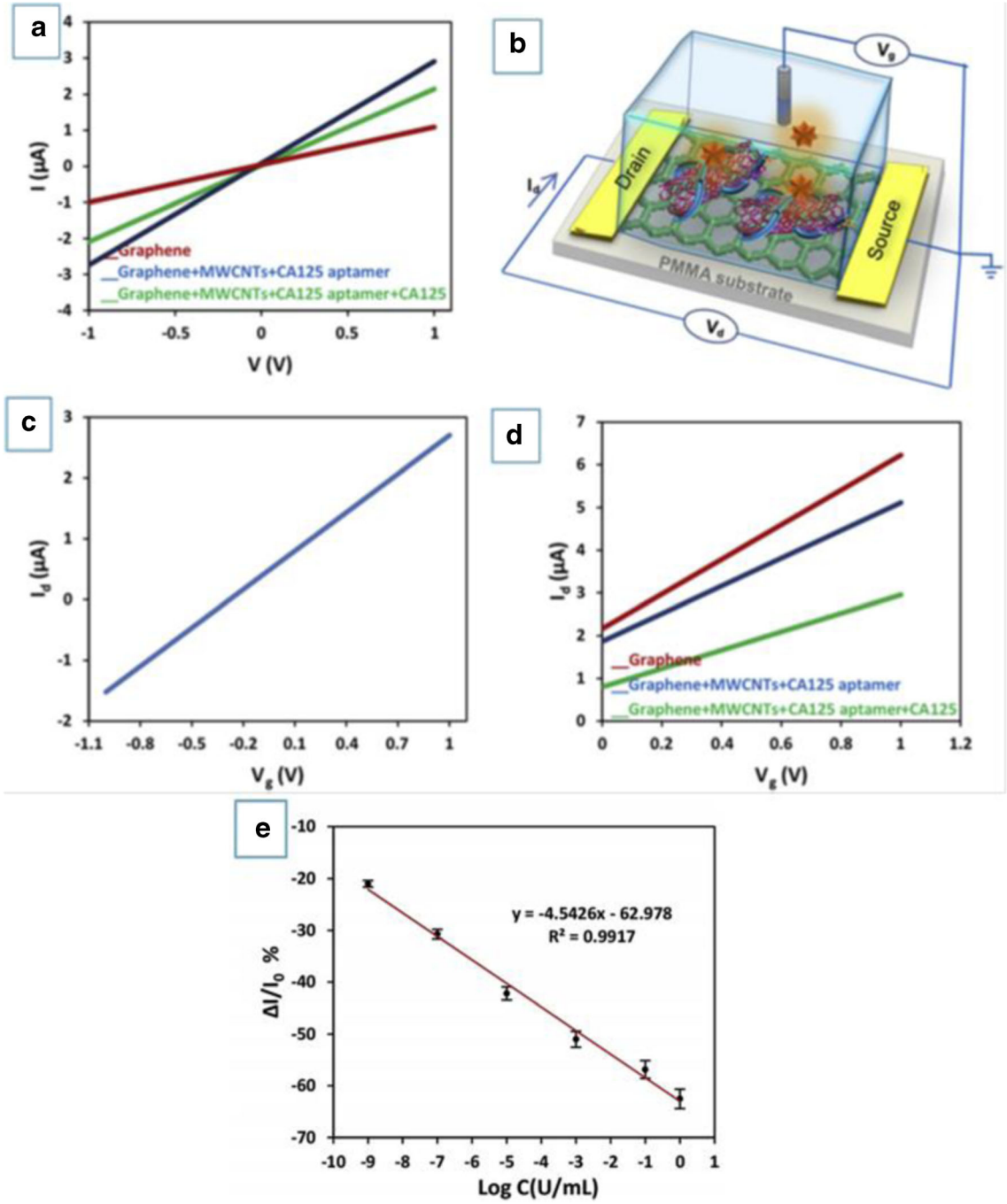

Fig. 4 **a** I–V responses of with and without MWCNTs modified with CA125 ssDNA and after CA125 incubation. **b** The flexible FET-based nanobiosensor. **c** The I_d–V_g result of the rGO FET aptasensor at Vd = 0.2 V. **d** Responses of the rGO FET nanosensor with and without MWCNTs modified with CA125 ssDNA and after CA125 incubation. **e** Calibration plot. Reprinted with the permission from [97]

Glutaraldehyde and EDC were covalently functionalized on the surface of single Ppy nanowire with CA125 Ab to fabricate a nanoimmunosensor for CA125 recognition. This sensor exhibited good sensitivity with relatively high limit of detection (1 U mL^{-1}) of CA125 over the linear region until 1000 U mL^{-1}.

Wang et al. [99] reported the field-effect enzymatic detection (FEED)–type HRP-labeled CA125 sensor using glutaraldehyde functionalized CNTs. When the conventional FET-based biosensor uses the FET to offer a reference current, this FEED method provides a voltage-controlled current magnification, generated using quantum tunneling of electrons, depending upon the distance of electrons traveled via tunneling and the potential energy profile. This sensor was able to detect 0.9 U mL^{-1} of CA125 which was high. Its applicability in real serum samples was not checked.

Giant magnetoresistive biosensor

Giant magnetoresistive (GMR) technique has been developed for biomolecular recognition based on determination of magnetically labeled targets as it exhibits several advantages like good sensitivity, compatibility with the integrated circuits (ICs), and potentiality for quantifying concentrations of manifold biomarkers all at once(viz., multiplex) in a transportable device [100]. Multiplexing is easy in GMR biosensing since the magnetic dipole fields remain confined to a small area near each sensor's surface and thus avoiding interference with the neighboring sensors.

Klein et al. [101] reported a multiplexed GMR biosensor array prototype to quantify CA125, HE4 wherein magnetoresistance signals were examined by a nearly balanced Wheatstone bridge circuit. Every single sensor was printed with the preferred antibodies that act as binding sites for the biomarkers in the multiplex assess towards concurrent measurements. The sensor displayed ultra-low limit of detection (3.7 U/mL, 7.4 pg/mL) towards sensing of CA125 and HE4, respectively.

A summary of the reported electrochemical and other methods employed in biosensing of ovarian cancer biomarkers is summarized in Table 2.

Conclusion and future perspectives

Timely recognition and prevention of ovarian cancer are the ultimate principles to achieve success in the entire cancer treatment process. Firstly, so far, a wide variety of biosensors have been reported in the literature towards determination of only CA125. Very few reports are available on recognition of other important biomarkers like HE4, prostasin. Therefore, substantial research needs to be done towards fabrication of biosensors for determination of HE4, prostasin. Secondly, at

Table 2 List of nanomaterials based biosensors towards determination of ovarian cancer biomarkers

Ovarian cancer biomarkers	Nanomaterials	Recognition methods	Detection limit	Linear range
CA125	Core–shell gold–Ag NPs	Electrochemical	-	1–150 IU mL^{-1} [63]
CA125	TbFe-based MOFs	Electrochemical	58 μU mL^{-1}	100 μU mL^{-1}–200 U mL^{-1} [64]
CA125	Gold nanostructure	Electrochemical	5.5 U mL^{-1}	10–100 U mL^{-1} [66]
CA125	Prussian Blue–Pt NPs polyaniline	Electrochemical	4.4 mU mL^{-1}	0.01–5000 U mL^{-1} [67]
CA125	Gold NP–ZnO nanorods	Electrochemical	2.5 ng μL^{-1}	2.5 ng μL^{-1}–1 μg μL^{-1} [68]
CA125	Graphene–polyaniline	Electrochemical	0.923 ng μL^{-1}	0.92 pg μL^{-1}–15.2 ng μL^{-1} [69]
CA125	Gold NPs	Electrochemical	6.7 U mL^{-1}	0–100 U mL^{-1} [70]
CA125	Ag NP–GQDs	Electrochemical	0.01 U mL^{-1}	- [71]
CA125	FA-HCl-doped polyaniline–chitosan and Ag–Co_3O_4 nanosheets	Electrochemical	0.25 pg mL^{-1}	0.001–25 ng mL^{-1} [72]
CA125	Chitosan–gold NP–CNT–GO	Electrochemical	0.002 U mL^{-1}	0.01–100 U mL^{-1} [73]
CA125	Poly-anthranilic acid–gold NP–Ag NPs	Electrochemical	2 U mL^{-1}	5–25 U mL^{-1} [74]
CA125	Hollow polydopamine–methylene blue	Electrochemical	0.336 μU mL^{-1}	0.01–100 U mL^{-1} [75]
CA125	Gold NPs	Electrochemical	1.73 U mL^{-1}	0–30 U mL^{-1} [76]
CA125	Porous carbon nanofiber	Electrochemical	1.8 U mL^{-1}	2–75 U mL^{-1} [77]
HE4	Gold NP–chitosan–TiC	Electrochemical	0.06 pM	0.06 pM
MUC1	Core–shell nanofiber–MWCNT–gold NPs	Electrochemical	2.7 nM	5–115 nM [79]
MUC1	Ag nanoclusters	Electrochemical	0.5 nM	1–500 nM [80]
CA125	Gold nanoelectrode	MIP	0.5 U mL^{-1}	0.5–400 U mL^{-1} [83]
CA125	PS imprinted CNT–Fe_2O_3 NP–polymer	MIP	0.49 U mL^{-1}	3.125–150 U mL^{-1} [84]
CA125	rGO–thionine–gold NPs	Paper-based electrochemical	0.01 U mL^{-1}	0.1–200 U mL^{-1} [88]
CA125	Chitosan–MWCNTs	Paper-based electrochemical	3.7 × 10–5 U mL^{-1}	1 × 10^{-4}–100 U mL^{-1} [89]
CA125	Ag–rGO/CysA–gold NPs	Paper-based electrochemical	0.78 U mL^{-1}	0.78–400 U mL^{-1} [90]
CA125	CNTs	Microfluidic, capacitive	-	-[92]
CA125	MoS2–gold nanoflowers	Microfluidic, electrochemical	0.36 pg mL^{-1}	0.01–50 ng mL^{-1} [93]
CA125	GO–chitosan–PGMA	Microfluidic, electrochemical	0.05 ng mL^{-1}	0.05–100 ng mL^{-1} [94]
CA125	MWCNT–rGO	Flexible FET type aptasensor	5 × 10–10 U mL^{-1}	1 × 10–9–1 U mL^{-1} [97]
CA125	Ppy nanowires	Chemiresistive	1 U mL^{-1}	1–1000 U mL^{-1} [98]
CA125	CNTs	FEED	0.9 U mL^{-1}	3–200 U mL^{-1} [99]

present, the ELISA is the only existing commercial recognition kit for ovarian cancer biomarker sensing that exhibits narrow detection range and low sensitivity. To eliminate these issues, the nanomaterial-based biosensors are advantageous as compared with the ELISA as they have the ability to be attached with aptasensors, thereby showing better sensitivity and selectivity. Thirdly, even if the optical biosensors resulted in favorable analytical consequences, most of them are involved in intricate, time-consuming arrangement which frequently failed to deliver a straightforward determination way of biomarkers. To tackle this, magnetoresistive, electrical, or electrochemical sensors exhibit enormous potential with their several benefits. Finally, still very few reports are presented on portable sensors to be employed outside the laboratory for recognition of ovarian cancer biomarkers. To commercialize the biosensors, incorporation of this biosensing platform into device level is essential that is still in early stages. To address it, current research towards fabrication of economical paper-based disposable biosensors or flexible FET type, GMR, or microfluidic-based lab-on-chip devices for determination of ovarian cancer biomarkers displays huge prospective.

In this regard, most of the recent pertinent articles were reviewed and corresponding analytical performances with sensing mechanisms for different biosensors were assessed. To conclude, exciting progresses are anticipated to take place in the near future for scaled-down sensing methodologies and testing kits that would pave a new avenue for ovarian cancer–affected patients to check their own health at ease.

Funding information SB receives financial assistance from the Scientific and Engineering Research Board (SERB) grant SB/WEA-03/2017.

Compliance with ethical standards

Conflict of interest The authors declare that they have no conflict of interest.

References

1. Matz M, Coleman MP, Sant M, Chirlaque MD, Visser O, Gore M et al (2017) The histology of ovarian cancer: worldwide distribution and implications for international survival comparisons (CONCORD-2). Gynecol Oncol 144(2):405–413
2. Zebrowski BK, Liu W, Ramirez K, Akagi Y, Mills GB, Ellis LM (1999) Markedly elevated levels of vascular endothelial growth factor in malignant ascites. Ann Surg Oncol 6(4):373
3. Numnum TM, Rocconi RP, Whitworth J, Barnes MN (2006) The use of bevacizumab to palliate symptomatic ascites in patients with refractory ovarian carcinoma. Gynecol Oncol 102(3):425–428
4. Bast RC, Hennessy B, Mills GB (2009) The biology of ovarian cancer: new opportunities for translation. Nat Rev Cancer 9(6):415–428
5. Badgwell D, Bast RC Jr (2007) Early detection of ovarian cancer. Dis Markers 23(5-6):397–410
6. Schink JC (1999) Semin Oncol 26(1 Suppl 1):2–7
7. Havrilesky LJ, Whitehead CM, Rubatt JM, Cheek RL, Groelke J, He Q et al (2008) Evaluation of biomarker panels for early stage ovarian cancer detection and monitoring for disease recurrence. Gynecol Oncol 110(3):374–382
8. Perfézou M, Turner A, Merkoçi A (2012) Cancer detection using nanoparticle-based sensors. Chem Soc Rev 41(7):2606–2622
9. Wang J (2005) Nanomaterial-based electrochemical biosensors. Analyst 130(4):421–426
10. Chen A, Chatterjee S (2013) Nanomaterials based electrochemical sensors for biomedical applications. Chem Soc Rev 42(12):5425–5438
11. Zhu C, Yang G, Li H, Du D, Lin Y (2015) Electrochemical sensors and biosensors based on nanomaterials and nanostructures. Anal Chem 87(1):230–249
12. Sha R, Badhulika S (2018) Facile synthesis of three-dimensional platinum nanoflowers decorated reduced graphene oxide: an ultra-high performance electro-catalyst for direct methanol fuel cells. Mater Sci Eng B 231:115–120
13. Sha R, Jones SS, Badhulika S (2019) Controlled synthesis of platinum nanoflowers supported on carbon quantum dots as a highly effective catalyst for methanol electro-oxidation. Surf Coat Technol 360:400–408
14. Razmi N, Hasanzadeh M (2018) Current advancement on diagnosis of ovarian cancer using biosensing of CA 125 biomarker: analytical approaches. TrAC Trends Anal Chem 108:1–12
15. Gupta D, Lis CG (2009) Role of CA125 in predicting ovarian cancer survival-a review of the epidemiological literature. J Ovarian Res 2(1):13
16. Diaconu I, Cristea C, Hârceagă V, Marrazza G, Berindan-Neagoe I, Săndulescu R (2013) Electrochemical immunosensors in breast and ovarian cancer. Clin Chim Acta 425:128–138
17. Bingle L, Singleton V, Bingle CD (2002) The putative ovarian tumour marker gene HE4 (WFDC2), is expressed in normal tissues and undergoes complex alternative splicing to yield multiple protein isoforms. Oncogene 21(17):2768–2773
18. Kirchhoff C (1998) Molecular characterization of epididymal proteins. Rev Reprod 3(2):86–95
19. Anastasi E, Granato T, Marchei GG, Viggiani V, Colaprisca B, Comploj S, Reale MG, Frati L, Midulla C (2010) Ovarian tumor marker HE4 is differently expressed during the phases of the menstrual cycle in healthy young women. Tumor Biol 31(5):411–415
20. Hellström I, Raycraft J, Hayden-Ledbetter M, Ledbetter JA, Schummer M, McIntosh M et al (2003) The HE4 (WFDC2) protein is a biomarker for ovarian carcinoma. Cancer Res 63(13):3695–3700
21. Montagnana M, Danese E, Giudici S, Franchi M, Guidi GC, Plebani M, Lippi G (2011) HE4 in ovarian cancer: from discovery to clinical application. Adv Clin Chem 55:2
22. Hellstrom I, Heagerty PJ, Swisher EM, Liu P, Jaffar J, Agnew K, Hellstrom KE (2010) Detection of the HE4 protein in urine as a biomarker for ovarian neoplasms. Cancer Lett 296(1):43–48
23. Huhtinen K, Suvitie P, Hiissa J, Junnila J, Huvila J, Kujari H et al (2009) Serum HE4 concentration differentiates malignant ovarian tumours from ovarian endometriotic cysts. Br J Cancer 100(8):1315–1319
24. Bast RC, Badgwell D, Lu Z, Marquez R, Rosen D, Liu J et al (2005) New tumor markers: CA125 and beyond. Int J Gynecol Cancer 15(Suppl 3):274–281
25. Wang W, Wang Y, Pan H, Cheddah S, Yan C (2019) Aptamer-based fluorometric determination for mucin 1 using gold nanoparticles and carbon dots. Microchim Acta 186(8):544
26. Wu S, Xu K, Chen G, Zhang J, Liu Z, Xie X (2012) Identification of serum biomarkers for ovarian cancer using MALDI–TOF-MS combined with magnetic beads. Int J Clin Oncol 17(2):89–95

27. Clarke CH, Yip C, Badgwell D, Fung ET, Coombes KR, Zhang Z et al (2011) Proteomic biomarkers apolipoprotein A1, truncated transthyretin and connective tissue activating protein III enhance the sensitivity of CA125 for detecting early stage epithelial ovarian cancer. Gynecol Oncol 122(3):548–553
28. Raamanathan A, Simmons GW, Christodoulides N, Floriano PN, Furmaga WB, Redding SW, Lu KH, Bast RC Jr, McDevitt JT (2012) Programmable bio-nano-chip systems for serum CA125 quantification: toward ovarian cancer diagnostics at the point-of-care. Cancer Prev Res 5(5):706–716
29. Ullah MF, Aatif M (2009) The footprints of cancer development: cancer biomarkers. Cancer Treat Rev 35(3):193–200
30. Scholler N, Crawford M, Sato A, Drescher CW, O'Briant KC, Kiviat N et al (2006) Bead-based ELISA for validation of ovarian cancer early detection markers. Clin Cancer Res 12(7):2117–2124
31. Wang S, Zhao X, Khimji I, Akbas R, Qiu W, Edwards D, Cramer DW, Ye B, Demirci U (2011) Integration of cell phone imaging with microchip ELISA to detect ovarian cancer HE4 biomarker in urine at the point-of-care. Lab Chip 11(20):3411–3418
32. Khan AH, Sadroddiny E (2016) Application of immuno-PCR for the detection of early stage cancer. Mol Cell Probes 30(2):106–112
33. Sood AK, Buller RE (1996) Genomic instability in ovarian cancer: a reassessment using an arbitrarily primed polymerase chain reaction. Oncogene 13(11):2499–2504
34. Celik N, Balachandran W, Manivannan N (2015) Graphene-based biosensors: methods, analysis and future perspectives. IET Circuits Devices Syst 9(6):434–445
35. Ramnani P, Saucedo NM, Mulchandani A (2016) Carbon nanomaterial-based electrochemical biosensors for label-free sensing of environmental pollutants. Chemosphere 143:85–98
36. Pumera M (2011) Graphene in biosensing. Mater Today 14(7–8): 308–315
37. Sha R, Badhulika S, Mulchandani A (2017) Graphene-based biosensors and their applications in biomedical and environmental monitoring. In: Label-free biosensing. Springer, Cham, pp 261–290
38. Sahatiya P, Sha R, Badhulika S (2019) Flexible 2D electronics in sensors and bioanalytical applications. Handbook of Flexible and Stretchable Electronics
39. Jin H, Gui R, Gong J, Huang W (2017) Aptamer and 5-fluorouracil dual-loading Ag2S quantum dots used as a sensitive label-free probe for near-infrared photoluminescence turn-on detection of CA125 antigen. Biosens Bioelectron 92:378–384
40. Wang J, Song J, Zheng H, Zheng X, Dai H, Hong Z, Lin Y (2019) Application of NiFe2O4 nanotubes as catalytically promoted sensing platform for ratiometric electrochemiluminescence analysis of ovarian cancer marker. Sensors Actuators B Chem 288:80–87
41. Bhatnagar D, Kumar V, Kumar A, Kaur I (2016) Graphene quantum dots FRET based sensor for early detection of heart attack in human. Biosens Bioelectron 79:495–499
42. Wei W, Li DF, Pan XH, Liu SQ (2012) Electrochemiluminescent detection of Mucin 1 protein and MCF-7 cancer cells based on the resonance energy transfer. Analyst 137(9):2101–2106
43. Hamd-Ghadareh S, Salimi A, Fathi F, Bahrami S (2017) An amplified comparative fluorescence resonance energy transfer immunosensing of CA125 tumor marker and ovarian cancer cells using green and economic carbon dots for bio-applications in labeling, imaging and sensing. Biosens Bioelectron 96:308–316
44. Ma N, Jiang W, Li T, Zhang Z, Qi H, Yang M (2015) Fluorescence aggregation assay for the protein biomarker mucin 1 using carbon dot-labeled antibodies and aptamers. Microchim Acta 182(1–2): 443–447
45. Yang X, Tang Y, Zhang X, Hu Y, Tang YY, Hu LY, Li S, Xie Y, Zhu D (2019) Fluorometric visualization of mucin 1 glycans on cell surfaces based on rolling-mediated cascade amplification and CdTe quantum dots. Microchim Acta 186(11):721
46. Li Z, Mao G, Du M, Tian S, Niu L, Ji X, He Z (2019) A fluorometric turn-on aptasensor for mucin 1 based on signal amplification via a hybridization chain reaction and the interaction between a luminescent ruthenium (II) complex and CdZnTeS quantum dots. Microchim Acta 186(4):233
47. Hasanzadeh M, Shadjou N (2017) What are the reasons for low use of graphene quantum dots in immunosensing of cancer biomarkers? Mater Sci Eng C 71:1313–1326
48. Zeng S, Hu S, Xia J, Anderson T, Dinh XQ, Meng XM et al (2015) Graphene–MoS2 hybrid nanostructures enhanced surface plasmon resonance biosensors. Sensors Actuators B Chem 207:801–810
49. Suwansa-ard S, Kanatharana P, Asawatreratanakul P, Wongkittisuksa B, Limsakul C, Thavarungkul P (2009) Comparison of surface plasmon resonance and capacitive immunosensors for cancer antigen 125 detection in human serum samples. Biosens Bioelectron 24(12):3436–3441
50. Zhang K, Shen X (2013) Cancer antigen 125 detection using the plasmon resonance scattering properties of gold nanorods. Analyst 138(6):1828–1834
51. Yuan J, Duan R, Yang H, Luo X, Xi M (2012) Detection of serum human epididymis secretory protein 4 in patients with ovarian cancer using a label-free biosensor based on localized surface plasmon resonance. Int J Nanomedicine 7:2921
52. Yang Z, Xie Z, Liu H, Yan F, Ju H (2008) Streptavidin-functionalized three-dimensional ordered nanoporous silica film for highly efficient chemiluminescent immunosensing. Adv Funct Mater 18(24):3991–3998
53. Al-Ogaidi I, Gou H, Aguilar ZP, Guo S, Melconian AK, Al-Kazaz AKA et al (2014) Detection of the ovarian cancer biomarker CA-125 using chemiluminescence resonance energy transfer to graphene quantum dots. Chem Commun 50(11):1344–1346
54. Babamiri B, Hallaj R, Salimi A (2018) Ultrasensitive electrochemiluminescence immunoassay for simultaneous determination of CA125 and CA15-3 tumor markers based on PAMAM-sulfanilic acid-Ru (bpy) 32+ and PAMAM-CdTe@CdS nanocomposite. Biosens Bioelectron 99:353–360
55. Tan X, Zhang B, Zhou J, Zou G (2017) Spectrum-based electrochemiluminescence immunoassay for selectively determining CA125 in greenish waveband. ChemElectroChem 4(7): 1714–1718
56. Wu L, Sha Y, Li W, Wang S, Guo Z, Zhou J et al (2016) One-step preparation of disposable multi-functionalized g-C3N4 based electrochemiluminescence immunosensor for the detection of CA125. Sensors Actuators B Chem 226:62–68
57. Sha R, Vishnu N, Badhulika S (2019) MoS2 based ultra-low-cost, flexible, non-enzymatic and non-invasive electrochemical sensor for highly selective detection of uric acid in human urine samples. Sensors Actuators B Chem 279:53–60
58. Deepika J, Sha R, Badhulika S (2019) A ruthenium (IV) disulfide based non-enzymatic sensor for selective and sensitive amperometric determination of dopamine. Microchim Acta 186(7):480
59. Sha R, Vishnu N, Badhulika S (2019) FeS2 grown pencil graphite as an in-expensive and non-enzymatic sensor for sensitive detection of uric acid in non-invasive samples. Electroanalysis 31(12): 2397–2403
60. Sha R, Durai L, Badhulika S (2018) Facile in-situ preparation of few-layered reduced graphene oxide–niobium pentoxide composite for non-enzymatic glucose monitoring. In: 2018 4th IEEE International Conference on Emerging Electronics (ICEE) (pp 1–4). IEEE
61. Sha R, Vishnu N, Badhulika S (2018) Bimetallic Pt-Pd nanostructures supported on MoS 2 as an ultra-high performance

electrocatalyst for methanol oxidation and nonenzymatic determination of hydrogen peroxide. Microchim Acta 185(8):399
62. Sha R, Gopalakrishnan A, Sreenivasulu KV, Srikanth VV, Badhulika S (2019) Template-cum-catalysis free synthesis of α-MnO2 nanorods-hierarchical MoS2 microspheres composite for ultra-sensitive and selective determination of nitrite. J Alloys Compd 794:26–34
63. Raghav R, Srivastava S (2015) Core–shell gold–silver nanoparticles based impedimetric immunosensor for cancer antigen CA125. Sensors Actuators B Chem 220:557–564
64. Wang M, Hu M, Li Z, He L, Song Y, Jia Q et al (2019) Construction of Tb-MOF-on-Fe-MOF conjugate as a novel platform for ultrasensitive detection of carbohydrate antigen 125 and living cancer cells. Biosens Bioelectron 142:111536
65. Johari-Ahar M, Rashidi MR, Barar J, Aghaie M, Mohammadnejad D, Ramazani A et al (2015) An ultrasensitive impedimetric immunosensor for detection of the serum oncomarker CA-125 in ovarian cancer patients. Nanoscale 7(8): 3768–3779
66. Torati SR, Kasturi KC, Lim B, Kim C (2017) Hierarchical gold nanostructures modified electrode for electrochemical detection of cancer antigen CA125. Sensors Actuators B Chem 243:64–71
67. Zheng Y, Wang H, Ma Z (2017) A nanocomposite containing Prussian Blue, platinum nanoparticles and polyaniline for multi-amplification of the signal of voltammetric immunosensors: highly sensitive detection of carcinoma antigen 125. Microchim Acta 184(11):4269–4277
68. Gasparotto G, Costa JPC, Costa PI, Zaghete MA, Mazon T (2017) Electrochemical immunosensor based on ZnO nanorods-Au nanoparticles nanohybrids for ovarian cancer antigen CA-125 detection. Mater Sci Eng C 76:1240–1247
69. Gazze A, Ademefun R, Conlan RS, Teixeira SR (2018) Electrochemical impedence spectroscopy enabled CA125 detection; toward early ovarian cancer diagnosis using graphene biosensors. J Interdiscipl Nanomed 3(2):82–88
70. Ravalli A, Dos Santos GP, Ferroni M, Faglia G, Yamanaka H, Marrazza G (2013) New label free CA125 detection based on gold nanostructured screen-printed electrode. Sensors Actuators B Chem 179:194–200
71. Jafari M, Hasanzadeh M, Solhi E, Hassanpour S, Shadjou N, Mokhtarzadeh A, Jouyban A, Mahboob S (2019) Ultrasensitive bioassay of epitope of Mucin-16 protein (CA 125) in human plasma samples using a novel immunoassay based on silver conductive nano-ink: a new platform in early stage diagnosis of ovarian cancer and efficient management. Int J Biol Macromol 126:1255–1265
72. Ren X, Wang H, Wu D, Fan D, Zhang Y, Du B, Wei Q (2015) Ultrasensitive immunoassay for CA125 detection using acid site compound as signal and enhancer. Talanta 144:535–541
73. Pakchin PS, Ghanbari H, Saber R, Omidi Y (2018) Electrochemical immunosensor based on chitosan-gold nanoparticle/carbon nanotube as a platform and lactate oxidase as a label for detection of CA125 oncomarker. Biosens Bioelectron 122:68–74
74. Taleat Z, Ravalli A, Mazloum-Ardakani M, Marrazza G (2013) CA 125 Immunosensor based on poly-anthranilic acid modified screen-printed electrodes. Electroanalysis 25(1):269–277
75. Liang X, Han H, Ma Z (2019) pH responsive amperometric immunoassay for carcinoma antigen 125 based on hollow polydopamine encapsulating methylene blue. Sensors Actuators B Chem 290:625–630
76. Wu L, Chen J, Du D, Ju H (2006) Electrochemical immunoassay for CA125 based on cellulose acetate stabilized antigen/colloidal gold nanoparticles membrane. Electrochim Acta 51(7):1208–1214
77. Wu L, Yan F, Ju H (2007) An amperometric immunosensor for separation-free immunoassay of CA125 based on its covalent immobilization coupled with thionine on carbon nanofiber. J Immunol Methods 322(1-2):12–19
78. Lu L, Liu B, Zhao Z, Ma C, Luo P, Liu C, Xie G (2012) Ultrasensitive electrochemical immunosensor for HE4 based on rolling circle amplification. Biosens Bioelectron 33(1):216–221
79. Paimard G, Shahlaei M, Moradipour P, Karamali V, Arkan E (2020) Impedimetric aptamer based determination of the tumor marker MUC1 by using electrospun core-shell nanofibers. Microchim Acta 187(1):5
80. Guo Q, Li X, Shen C, Zhang S, Qi H, Li T, Yang M (2015) Electrochemical immunoassay for the protein biomarker mucin 1 and for MCF-7 cancer cells based on signal enhancement by silver nanoclusters. Microchim Acta 182(7–8):1483–1489
81. Wang Y, Zhang Z, Jain V, Yi J, Mueller S, Sokolov J et al (2010) Potentiometric sensors based on surface molecular imprinting: detection of cancer biomarkers and viruses. Sensors Actuators B Chem 146(1):381–387
82. Badhulika S, Mulchandani A (2015) Molecular imprinted polymer functionalized carbon nanotube sensors for detection of saccharides. Appl Phys Lett 107(9):093107
83. Viswanathan S, Rani C, Ribeiro S, Delerue-Matos C (2012) Molecular imprinted nanoelectrodes for ultra sensitive detection of ovarian cancer marker. Biosens Bioelectron 33(1):179–183
84. Büyüktiryaki S, Say R, Denizli A, Ersöz A (2017) Phosphoserine imprinted nanosensor for detection of Cancer Antigen 125. Talanta 167:172–180
85. Hu J, Wang S, Wang L, Li F, Pingguan-Murphy B, Lu TJ, Xu F (2014) Advances in paper-based point-of-care diagnostics. Biosens Bioelectron 54:585–597
86. Wang Y, Xu H, Luo J, Liu J, Wang L, Fan Y et al (2016) A novel label-free microfluidic paper-based immunosensor for highly sensitive electrochemical detection of carcinoembryonic antigen. Biosens Bioelectron 83:319–326
87. Dungchai W, Chailapakul O, Henry CS (2011) A low-cost, simple, and rapid fabrication method for paper-based microfluidics using wax screen-printing. Analyst 136(1):77–82
88. Fan Y, Shi S, Ma J, Guo Y (2019) A paper-based electrochemical immunosensor with reduced graphene oxide/thionine/gold nanoparticles nanocomposites modification for the detection of cancer antigen 125. Biosens Bioelectron 135:1–7
89. Ge S, Ge L, Yan M, Song X, Yu J, Huang J (2012) A disposable paper-based electrochemical sensor with an addressable electrode array for cancer screening. Chem Commun 48(75):9397–9399
90. Bahavarnia F, Saadati A, Hassanpour S, Hasanzadeh M, Shadjou N, Hassanzadeh A (2019) Paper based immunosensing of ovarian cancer tumor protein CA 125 using novel nano-ink: a new platform for efficient diagnosis of cancer and biomedical analysis using microfluidic paper-based analytical devices (μPAD). Int J Biol Macromol 138:744–754
91. Lafleur JP, Jönsson A, Senkbeil S, Kutter JP (2016) Recent advances in lab-on-a-chip for biosensing applications. Biosens Bioelectron 76:213–233
92. Mandal D, Nunna BB, Zhuang S, Rakshit S, Lee ES (2018) Carbon nanotubes based biosensor for detection of cancer antigens (CA-125) under shear flow condition. Nano-Struct Nano-Objects 15:180–185
93. Wang X, Deng W, Shen L, Yan M, Yu J (2016) A 3D electrochemical immunodevice based on an Au paper electrode and using Au nanoflowers for amplification. New J Chem 40(3):2835–2842
94. Wu Y, Xue P, Hui KM, Kang Y (2014) A paper-based microfluidic electrochemical immunodevice integrated with amplification-by-polymerization for the ultrasensitive multiplexed detection of cancer biomarkers. Biosens Bioelectron 52:180–187

95. Nunna BB, Mandal D, Lee JU, Singh H, Zhuang S, Misra D, Bhuyian MNU, Lee ES (2019) Detection of cancer antigens (CA-125) using gold nano particles on interdigitated electrode-based microfluidic biosensor. Nano Converg 6(1):3
96. Zhao Z, Yang Y, Zeng Y, He M (2016) A microfluidic ExoSearch chip for multiplexed exosome detection towards blood-based ovarian cancer diagnosis. Lab Chip 16(3):489–496
97. Majd SM, Salimi A (2018) Ultrasensitive flexible FET-type aptasensor for CA 125 cancer marker detection based on carboxylated multiwalled carbon nanotubes immobilized onto reduced graphene oxide film. Anal Chim Acta 1000:273–282
98. Bangar MA, Shirale DJ, Chen W, Myung NV, Mulchandani A (2009) Single conducting polymer nanowire chemiresistive label-free immunosensor for cancer biomarker. Anal Chem 81(6):2168–2175
99. Wang J, Yau ST (2011) Field-effect amperometric immunodetection of protein biomarker. Biosens Bioelectron 29(1):210–214
100. Costa T, Cardoso FA, Germano J, Freitas PP, Piedade MS (2017) A CMOS front-end with integrated magnetoresistive sensors for biomolecular recognition detection applications. IEEE Trans Biomed Circuits Syst 11(5):988–1000
101. Klein T, Wang W, Yu L, Wu K, Boylan KL, Vogel RI et al (2019) Development of a multiplexed giant magnetoresistive biosensor array prototype to quantify ovarian cancer biomarkers. Biosens Bioelectron 126:301–307